Earth and Space Science

TECHNICAL REPORTS: METHODS

10.1029/2021EA001789

Depth Estimation of Potential Field by Using a New Downward Continuation Based on the Continued Fraction in Space Domain

Wenna Zhou[1], Chong Zhang[2,3], and Dailei Zhang[2,4]

[1]School of Earth Sciences, Key Laboratory of Mineral Resources in Western China (Gansu Province), Lanzhou University, Lanzhou, Gansu, China, [2]China Deep Exploration Center (SinoProbe Center), Chinese Academy of Geological Sciences, Beijing, China, [3]Chengdu Center, China Geological Survey, Chengdu, Sichuan Province, China, [4]Geothermal and Hot Dry Rock Exploration and Development Technology Innovation Center of the Ministry of Natural Resources, Shijiazhuang, Hebei, China

Key Points:

- Downward continuation method based on continued fraction in space domain is proposed
- Depth information can be obtained by the new downward continuation method directly
- Continued fraction would be a new powerful tool to processing potential field data

Correspondence to:

W. Zhou and C. Zhang,
wennazhou@163.com;
zchong_chn@163.com

Citation:

Zhou, W., Zhang, C., & Zhang, D. (2021). Depth estimation of potential field by using a new downward continuation based on the continued fraction in space domain. *Earth and Space Science*, *8*, e2021EA001789. https://doi.org/10.1029/2021EA001789

Received 31 MAR 2021
Accepted 28 MAY 2021

Abstract Depth estimation of potential field data is a powerful tool for geologic source interpretation. It can be implemented by using downward continuation method based on a normalized algorithm. However, when several geological bodies with different burial depths exist in the research area, the calculated depth usually tends to be the average depth. To overcome this limitation, we proposed a new downward continuation method based on the relationship between the Taylor series and the continued fraction in space domain. Theoretically, it can obtain the singular (quasi-singular) source point directly, which indicates the position of source. In practical applications, we only need to calculate downward continuation data from the original level to an expected maximum depth. The absolute value is calculated so that the maximum value indicates the source depth range. We used different synthetic models to test our method and obtained satisfactory results. The advantages of depth estimation using the new method were illustrated by comparing it with the normalized total gradient method. Finally, we applied the new method to field data, and results were in agreement with the previous results. This illustrated that the new method can be used for high resolution, high accuracy depth estimation.

1. Introduction

Interpretation of potential field data plays an important role in the study of geologic structure and resource exploration. The advantage of potential field data is its lateral resolution, and horizontal positions can be pinpointed. In many applications, however, researchers are often interested in depth information rather than other parameters such as dimension and physical property contrast. Thus, various depth estimation methods have been developed. Li (2003) summarized and compared the most common classical methods, including Euler deconvolution (Stavrev & Reid, 2007, 2010; Thompson, 1982), Naudy method (Naudy, 1971), Werner deconvolution (Hansen, 2005; Hartman et al., 1971), analytic signal-based methods (Bastani & Pedersen, 2001; Nabighian, 1972; Roest et al., 1992), local wavenumber methods (Keating, 2009; Thurston & Smith, 1997), and wavelets methods (Cooper, 2006). These methods are very useful and effective in potential field data depth interpretation.

Along with the developments of airborne gravity and magnetic measurements, researchers are paying more attention to multiscale methods, which use the data of different levels. Analytic continuation is the most common and effective strategy to implement these methods. Many multiscale techniques have been proposed using upward continuation because of its stability, such as DEXP, ScalFun, the reduced and multiridge Euler (Abbas & Fedi, 2014; Cella et al., 2009; Fedi et al., 2009, 2012, 2015; Florio & Fedi, 2014; Zhou, 2016; Zhou et al., 2016). Florio and Fedi (2018) gave a simple summary about these methods. Fedi et al. (2009) pointed out that these methods can recover the resolution that is lost with the increased altitude by combining the transformation with high order vertical differentiations. However, it is still difficult to distinguish the information greater burial depths.

Conversely, it is well known that downward continuation can be used to enhance the resolution of gravity and magnetic field data. However, this inherently unstable feature has limited widespread applications. Although numerous methods have been proposed to improve the calculation stability and accuracy (Pašteka et al., 2012; Pilkington & Boulanger, 2017; Xu et al., 2007; Zeng et al., 2013; Zhang et al., 2013, 2018; Zhou et al., 2018), downward continuation methods are not developed enough to over cover depths equal to or greater than the depth at which the field becomes singular (Fedi & Florio, 2011). Therefore, depth estimation methods based on downward continuation, such as the normalized total gradient (NTG) and the singular (quasi-singular) point method, usually require additional calculations (Elysseieva & Pašteka, 2009, 2019; Fedi & Florio, 2011). In fact, these methods are similar in basic normalized theory. There also are many modified methods that obtain more precise and robust results (Ermokhine & Efimova, 2006; Fedi & Florio, 2011; Zeng et al., 2002; Zhou, 2015). However, their accuracy mainly depends on the stability of the original downward continuation method. The depth estimation error is very obvious when the spatial measured distance between the different geologic sources is small.

In this paper, we proposed a new downward continuation method based on the continued fraction. We deduced our new equation from the Taylor series in space domain and only needed to calculate downward continuation from the original level to an expected maximum level. The positions of singular (quasi-singular) points can be detected, which usually can be used to indicate the positions of source. The singularity comes about because of the choice of kernel or attempting to continue the field inside the source. Thus, the source depth was directly obtained without any normalized calculations. Different model data with and without noise were used to test the practical application effect of our new method. Finally, the new method was applied to real gravity data.

2. Theory

2.1. Downward Continuation Based on the Continued Fraction

It is well known that the downward continuation algorithm is unstable and will enhance noise as well as detail. To overcome the limitation, Taylor series expansion is usually used to improve the stability (Fedi & Florio, 2002; Ma et al., 2013; Wang et al., 2011; Zhang et al., 2013). However, Taylor series expansion is not the best approximation function. Zhou et al. (2018) compared different approximation function and pointed out that superior approximation function can be used to get more accurate downward continuation results.

Continued fractions are connected with interpolation and approximation problems. It has been proved the computational accuracy and convergence rate has its corresponding advantages (Lee & Kim, 2011; Li & Chen, 2015). Therefore, we use the continued fraction to establish a downward continuation method aim to bring the advantage. An ordinary continued fraction (CF) is an expression of the form (Cuyt & Verdonk, 1988)

$$b_0 + \cfrac{a_1}{b_1 + \cfrac{a_2}{b_2 + \cfrac{a_3}{b_3 + \cdots}}}, \tag{1}$$

which is often written in a more convenient way

$$b_0 + \sum_{i=1}^{\infty} \frac{a_i \mid}{\mid b_i}. \tag{2}$$

To establish the relationship between the Taylor series and the continued fraction, the continued fraction first needs to be introduced. Based on Equation 1, the Thiele continued fraction for a rational function $f(z)$ is written as (Cuyt & Verdonk, 1988; Li et al., 2008)

$$f(z) = b_0 + \cfrac{z - z_0}{b_1 + \cfrac{z - z_1}{b_2 + \cfrac{z - z_2}{b_3 + \ldots}}}. \tag{3}$$

The Pringsheim continued fraction form can be rewritten as

$$f(z) = b_0 + \frac{z - z_0 \mid}{\mid b_1} + \frac{z - z_1 \mid}{\mid b_2} + \ldots + \frac{z - z_{n-1} \mid}{\mid b_n} + \ldots, \tag{4}$$

where the notation $\frac{|}{|}$ is the Pringsheim form.

The downward continuation based on a truncated Taylor series in space domain has been introduced by various authors (Evjen, 1936; Fedi & Florio, 2002). It can be written as

$$\begin{aligned} f(x,y,z) &= f(x,y,z_0) + \left[\frac{\partial f}{\partial z}\right]_{z_0}(z-z_0) + \frac{1}{2!}\left[\frac{\partial^2 f}{\partial z^2}\right]_{z_0}(z-z_0)^2 \\ &+ \ldots + \frac{1}{m!}\left[\frac{\partial^m f}{\partial z^m}\right]_{z_0}(z-z_0)^m \end{aligned}, \tag{5}$$

where $f(x, y, z)$ is the potential field, z_0 is the measurement level, z is the continuation level, and m is the number of terms in the Taylor series.

The relationship between the Taylor series and the continued fraction can be written as (Cuyt & Verdonk, 1988; Li et al., 2008)

$$f(z) = \sum_{i=0}^{\infty} C_i^{(0)}(z-z_0)^i = b_0 + \frac{z-z_0\,|}{|\,b_1} + \frac{z-z_0\,|}{|\,b_2} + \ldots, \tag{6}$$

where

$$C_i^{(0)} = \frac{f^{(i)}(z_0)}{i!}, i = 0,1,2,\ldots. \tag{7}$$

In order to establish a relationship between the Taylor series and the continued fraction, the coefficients can be obtained through the Viscovatov algorithm as follows (Cuyt & Verdonk, 1988; Li et al., 2008)

$$\begin{cases} b_0 = C_0^{(0)}; \\ b_1 = 1 / C_1^{(0)}; \\ C_i^{(1)} = -C_{i+1}^{(0)} / C_1^{(0)}, i \ge 1; \\ b_l = C_1^{(l-2)} / C_1^{(l-1)}, l \ge 2; \\ C_i^{(l)} = C_{i+1}^{(l-2)} - b_l C_{i+1}^{(l-1)}, i \ge 1, l \ge 2. \end{cases}, \tag{8}$$

where the index l also is a positive integer.

From Equation 7, we obtain

$$\begin{cases} C_0^{(0)} = f(x,y,z_0); \\ C_1^{(0)} = \left[\frac{\partial f(x,y,z_0)}{\partial z}\right]_{z_0}; \\ C_2^{(0)} = \frac{1}{2!}\left[\frac{\partial^2 f(x,y,z_0)}{\partial z^2}\right]_{z_0}; \\ C_3^{(0)} = \frac{1}{3!}\left[\frac{\partial^3 f(x,y,z_0)}{\partial z^3}\right]_{z_0}; \\ \ldots \\ C_n^{(0)} = \frac{1}{n!}\left[\frac{\partial^n f(x,y,z_0)}{\partial z^n}\right]_{z_0} \end{cases}. \tag{9}$$

Coefficient of b_0, b_1, b_2, ... can be deduced from Equation 8, then the downward continuation based on continued fraction can be deduced from Equations 8 and 9:

$$f(x,y,z) = b_0 + \frac{z - z_0 \mid}{\mid b_1} + \frac{z - z_0 \mid}{\mid b_2} + ... \tag{10}$$

Similar to the downward continuation based on a Taylor series expansion, z_0 is the measurement level and z is the continuation level. Meanwhile, the appropriate terms for the continued fraction need to be selected. The more term corresponds to a higher-order derivative and it is highly sensitive to noise.

In Equation 10, the coefficients b_0, b_1, b_2 ... are higher-order derivatives and contain zero values. It is well known that division by zero or a very small number will produce individual random errors or infinite values in the result. To reduce this limitation, we applied a median filter with a 3×3 window to improve the results from Equation 10. The filter can be implemented using the filtering toolbox in MATLAB (Lim, 1990) to reduce the individual random error and preserve the main character of the results. Thus, we were able to calculate the downward continuation values using Equation 10 with simple filtering.

2.2. Depth Estimation Theory for Models

To illustrate the reason for the new method can be used to estimate the depth of source, we first used simple models to illustrate the theoretical differences between the classical Taylor method and the new method. Schematic figure (Figure 1) is presented to show the synthetic representation of the sphere and cylinder. All the parameters can be found in the equations of follows:

The infinite horizontal cylinder model is the simplest model to deduce the formula and was used to establish the NTG method. Therefore, we used the model to illustrate the new method. The gravity anomaly of an infinite horizontal cylinder can be written as (Gupta, 1983)

$$g(x,h) = 2 \cdot G \cdot \sigma \cdot \pi \cdot R^2 \frac{h}{h^2 + x^2}, \tag{11}$$

where G is the Newtonian constant, σ is the density contrast, R is the radius, and h is the depth of source. In order to represent the equations conveniently, we use $\lambda = \sigma \cdot \pi \cdot R^2$ to denote the mass of source. Then, we calculate the downward continuation value at depth of z, i.e., the gravity anomaly at the depth z can be written as

$$g(x,z) = 2 \cdot G \cdot \lambda \frac{h - z}{(h - z)^2 + x^2}, \tag{12}$$

When $x = 0$, Equation 12 can be simplified as

$$g(z) = 2 \cdot G \cdot \lambda \frac{1}{h - z}, \tag{13}$$

Theoretically, from the model formula, we can get the singular point when downward continuation data close the depth $z = h$ are obtained. It means if h has been set, we calculated different $g(z)$ from original level to a maximum depth, the singular (quasi-singular) point can be found. However, the downward continuation is very instable and usually cannot downward continued close the source depth. Meanwhile, we cannot denote the real data by using a theoretical model formula. Therefore, we cannot get the theoretically formula to find the singular point by using ordinary downward continuation method. The field data were simulated in the form of polynomials, Taylor or Fourier series. The downward continuation also was calculated by using different approximation or series function. Taylor series plays a very important role in this field. Here, we compare the new method with Taylor series to illustrate the superiority.

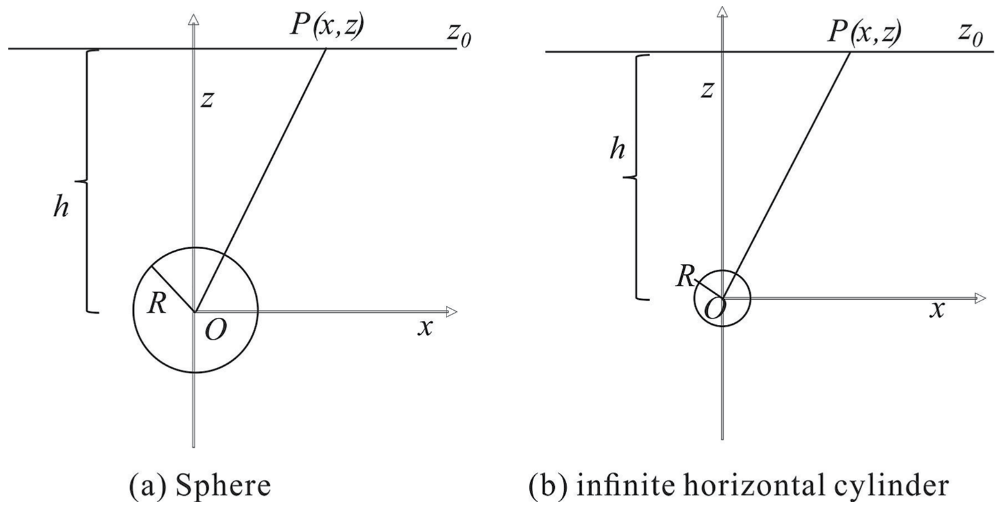

Figure 1. Schematic figure of sphere and infinite horizontal cylinder.

The downward continuation can be calculated by using the Taylor series

$$f\left(z\right) = 2 \cdot G \cdot \lambda \frac{1}{h}\left(1 + \frac{z}{h} + \left(\frac{z}{h}\right)^2 + \cdots + \left(\frac{z}{h}\right)^m\right), \tag{14}$$

where z is the continuation level, h is the depth of source, m is the term of Taylor series and it is a finite number. As z increases, the value of f will keep increasing. Therefore, the downward continuation method based on the Taylor series cannot display the source position. If we want to obtain the depth information (the singular point) by using Taylor series, the term of m must be infinite ∞. It is conflict with the finite potential filed data we measured or modeled, and it is very difficult to implement the method using infinite m. To overcome the limitation, a normalized algorithm was proposed (Elysseieva & Pašteka, 2009, 2019).

For the new continued fraction method, downward continuation can be calculated by using equation from Equations 6–10

$$f\left(z\right) = 2 \cdot G \cdot \lambda \cdot \frac{1}{h}\left(1 + \cfrac{z}{h + \cfrac{z}{-1}}\right). \tag{15}$$

Equation 15 can be translated as

$$f\left(z\right) \cdot \frac{h}{2G\lambda} - 1 = \frac{z}{h - z}, \tag{16}$$

and we can obtain the relationship of h and z

$$z = h - \frac{2G\lambda}{f\left(x\right)}. \tag{17}$$

It means when the downward continuation value close to the infinite, i.e., $f\left(x\right) \to \infty$, z is a finite value. Therefore, we can get $z = h$, when $\lim_{f(x)\to\infty}\left(h - \frac{2G\lambda}{f\left(x\right)}\right) = h$. Thus, the singular point can be obtained by using the new method at the depth $z = h$, which means the downward continuation data $f\left(z\right) \to \infty$.

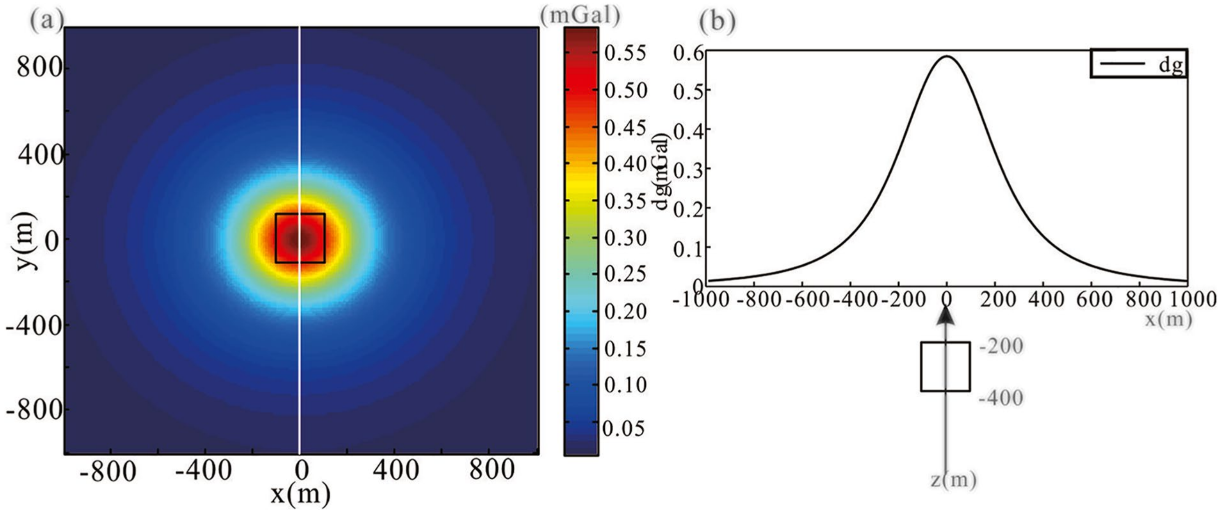

Figure 2. (a) The gravity effect of the prism model, which with a density of 1,000 kg/m^3 is buried at a depth from 200 to 400 m, where the black rectangle is the horizontal location of the prism, the white line is the position of cross section for $y = 0$ m. (b) The gravity anomaly of the vertical cross section for the coordinate $y = 0$ m, where the rectangle is the vertical location of the prism.

It is obvious that Equation 15 has the same form of Equation 13. In fact, for Equation 13, we can obtain the result by using only two terms of continued fraction downward continuation. When more terms are used to calculate, we need to use the limiting form, and the limiting results are the same as Equation 15. It means the downward continuation by using the new method, versus the classical Taylor series method, can approach the theoretical formula Equation 13, i.e., the new method can remain the characteristic of theoretical formula or the original data. In addition, from Equation 17, we can get the singular point by using the new method, where the downward continuation data close the depth $z = h$. It illustrates that the new method can be used to obtain the singular point within a finite number of terms. Therefore, relative to the classical NTG method, we can use this method to derive the depth of the source without normalized algorithm. Similar as the infinite horizontal cylinder gravity model, for the sphere model, we also can derive similar equations using the relationship between the Taylor series and the continued fraction method. In additional, we can get the similar results for the magnetic model.

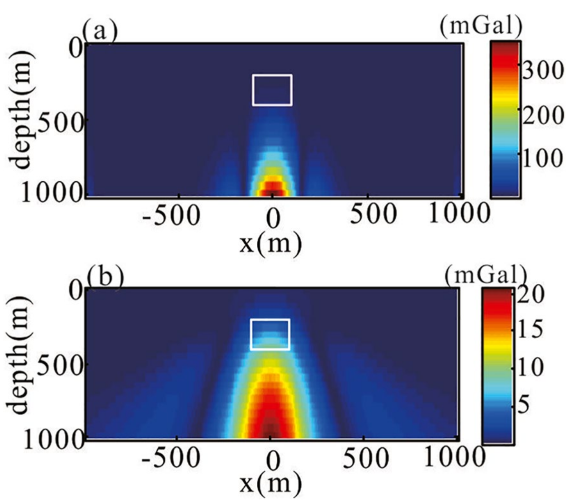

Figure 3. Cross section intersected from the 3D results of the classical downward continuation from 0 to 1,000 m, where the white rectangle is the position of the prism. (a) Result of DCISVD method and (b) result of the IDCFFT method.

In order to obtain the depth information, we must calculate the value below the source. An expected maximum level needs to be set that is greater than the source depth. However, a limiting case for downward continuation would be the top level of the sources (Fedi & Florio, 2011). To downward continue below the source is not valid from a strictly theoretical point of view in potential field theory. In the case of the continuation of discrete potential field functions, the potential field can numerically continue to arbitrary large depths (Pašteka et al., 2012, and references therein). Therefore, we only calculate the theoretical field to obtain information about source positions in the context of a numerical approximation rather than the continued field itself. Thus, to indicate the source position, we need to calculate the downward continuation from the original level to the expected maximum level using Equation 10, and then calculate the absolute value. The advantage of the new method is that it is no longer necessary to calculate the normalization value, which avoids the error produced by the normalized method and simplifies the calculation procedure.

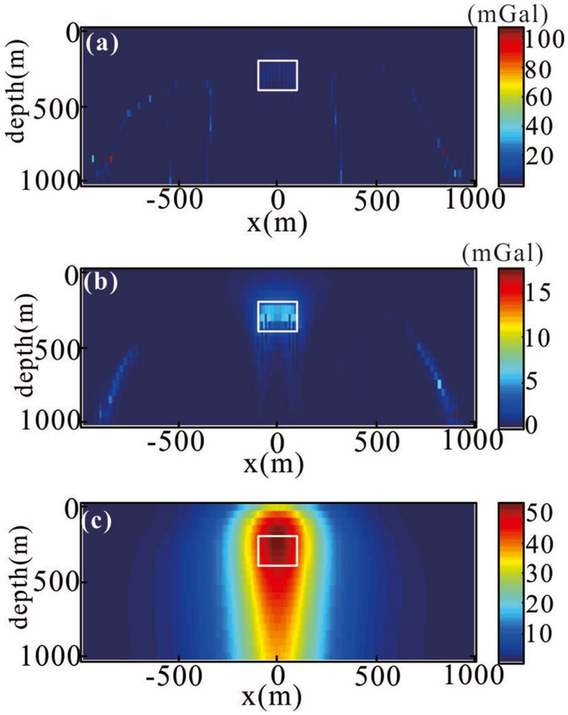

Figure 4. Cross section intersected from the 3D results of the proposed method and NTG from 0 to 1,000 m, where the white rectangle is the position of the prism. (a) Result of the proposed method without filtering, (b) result of the proposed method with median filtering, and (c) result of the NTG method. NTG, normalized total gradient.

3. Model Tests

3.1. A Simple Prism Model

A simple prism model was utilized to investigate the application effects of the new method. A prism with a density of 1,000 kg/m^3 was buried at a depth ranging from −200 m to −400 m. The horizontal position is shown in Figure 2a. The size and vertical positions of the prism are shown in Figure 2b (the rectangle in the figure). The sampling interval was 10 m. Figure 2a shows the gravity effects of the model.

To illustrate the remarkable features of the new method, we calculated the downward continued data from 0 to −1,000 m with a depth interval of 50 m using the different methods. To better display the results, a cross section (the white line in Figure 2) was intersected with the 3D results. Figures 3a and 3b show the results from the classical methods (the stable downward continuation method based on the integrated second vertical derivative (ISVD) in space domain (DCISVD) (Fedi & Florio, 2002) and the iteration downward continuation method based on FFT in the frequency domain (IDCFFT) (Xu et al., 2007)), respectively. They clearly show the value increasing with depth, while the depth information cannot be displayed. For the new method, we calculated the downward continued data using the same parameters and the absolute value is calculated further. Figure 4a displays the results without median filtering and the depth information already can be displayed. However, as described in theory section, there were many random errors or infinite values in the results. Therefore, we used a median filter with a 3 × 3 window to improve them, which are shown in Figure 4b. The maximum value corresponded with the position of the prism. This showed that the new method can be used to estimate the geologic source depth range. In this model test, median filtering was a tool used to eliminate the random errors or infinite values, and the depth information cannot be changed.

For comparison's sake, the NTG method was also used to obtain depth information in this section. We used an improved NTG method to calculate depth, which was established using an adaptive iterative downward continuation method (Zhou, 2015). The 2D cross section result is shown in Figure 4c. It can be seen that based on this simple situation, both the NTG method and the proposed method can be utilized to obtain depth information.

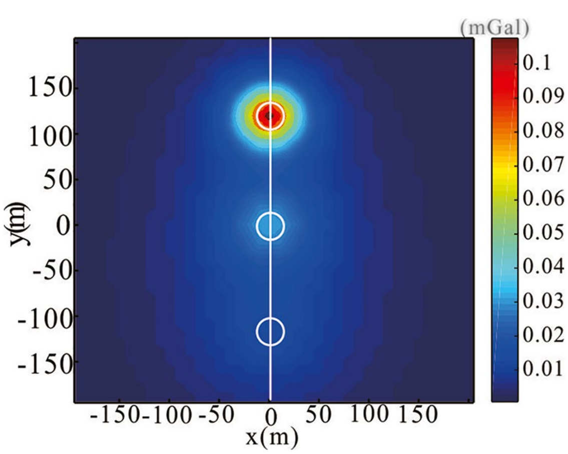

Figure 5. The gravity data of three spheres, where the white line is the position of cross section.

3.2. Model 2 With Three Spheres

To further test the capacity of depth estimation of the new method, we used three spheres with different depths. The spheres with a density of 1,000 kg/m^3 were buried at depths of 30 m (sphere 1), 60 m (sphere 2), and 90 m (sphere 3) and with respective horizontal coordinates of (0, 120), (0, 0), and (0, −120). The spheres all had the same radius of 15 m and the sampling interval was 10 m. The gravity anomalies are shown in Figure 5. We calculated the downward continuation from 0 to 120 m with a depth interval of 5 m, along with absolute values. To better display the results, we intersected a cross section with the 3D results. The cross section results are shown in Figure 6a, where white dots represent the maximum values. The actual positions of the spheres are indicated by the white circles. It can be seen that the spheres 1 and 2 were accurately located. Due to the shallow source effects, sphere 3 was slightly offset. Although the complex model contained three spheres with different depths, we obtained depth information for all the sources. The result

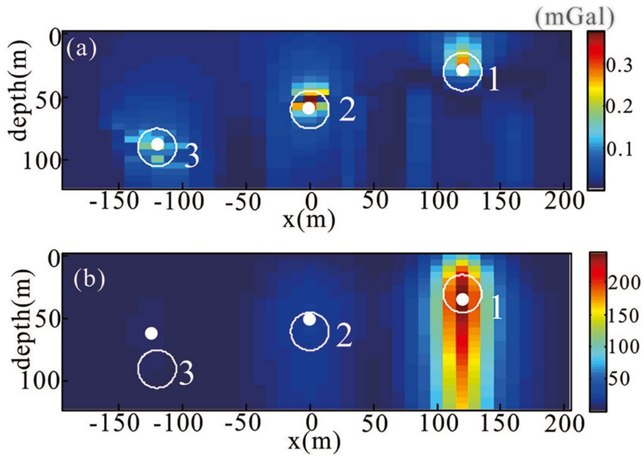

Figure 6. The cross section results from 0 to 120 m of gravity anomaly, where the white circles are the real positions of spheres and the white dots are the maximum values. (a) The result of the new method and (b) the result of NTG method. NTG, normalized total gradient.

of the improved NTG (Zhou, 2015) is shown in Figure 6b. It can be seen that all depths tended to be equal to 60 m, which was the average depth. This is the limitation of a normalized algorithm. For the complex model, the influence of different models was very evident. By comparison, therefore, the new method showed clear advantages of having simpler calculations with higher accuracy.

To further test the applicability of the new method, we simulated noise-corrupted data. The noise source was 0-mean Gaussian random noise with a standard deviation of 0.002 mGal, which was 2% of the maximum amplitude (Figure 5). It was added to the gravity data (Figure 7) and the new method was used to calculate the depth. Figure 7a shows the results using the data with noise. The depth of sphere 1 was still accurate, but the depths for spheres 2 and 3 were not displayed accurately. Especially, in this case, the depth information for sphere 3 almost cannot been obtained.

To improve the results, a simple Wiener filter with a 3 × 3 window size was used to process the original data in MATLAB, which is minimized the mean square error between the estimated random process and the desired process. The filtered gravity anomaly is shown in Figure 7b. Improved results were obtained based on the filtered data (Figure 8b). It can be seen that both the spheres 1 and 2 were displayed accurately. The depth information for sphere 3 still could not be displayed, perhaps because the signal is drowned by the noise. The new approach was established based on higher-order derivatives and is sensitive to noise. Therefore, before the method is used to calculate the depth range, it is necessary to filter the data to reduce noise effects.

4. Real Data Application

In the previous sections, we illustrated the applicability of the new method using different test examples. Now we will use a real test case of gravity data from the Vinton Salt Dome, Louisiana, USA. The Vinton Dome is characterized by stocks of Jurassic salt and intervening Cenozoic shelf mini-basins (Jackson et al., 1995). It consists of a core of massive salt and a well-defined cap rock extending above the salt rock (Coker et al., 2007). This cap rock successively grades downward from limestone to gypsum and anhydrite. Many authors have used full tensor gradient (FTG) data to test their new methods and to interpret the Vinton Salt Dome (Geng et al., 2014; Oliveira & Barbosa, 2013; Qin et al., 2019; Salem

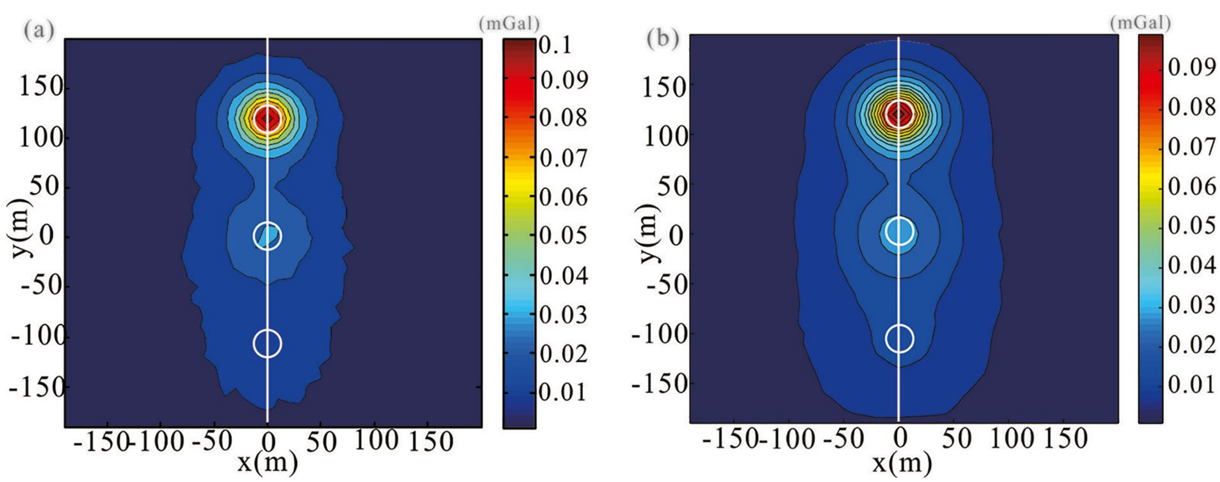

Figure 7. (a) The gravity anomaly with noise; (b) the filtered gravity anomaly by Wiener filter with a 3 × 3 window size, where the white line is the position of cross section.

10.1029/2021EA001789

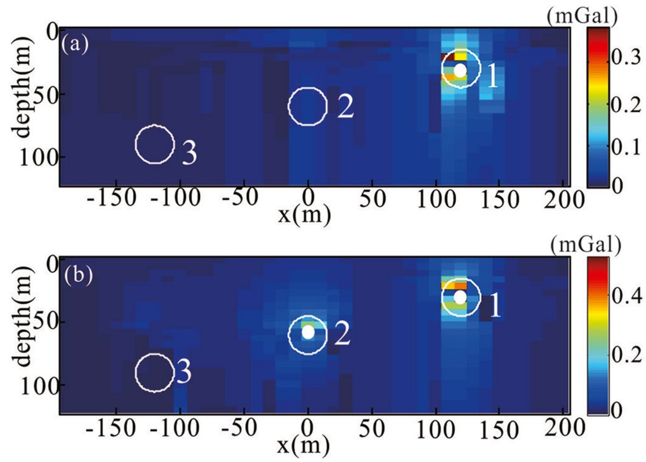

Figure 8. The cross section results from 0 to 120 m of the gravity anomaly with noise, where the white circles are the real positions of spheres and the white dots are the maximum values. (a) Result of gravity anomaly with noise and (b) result of gravity anomaly with noise processed by using a filter.

et al., 2013; Zhou, 2015; Zhou & Liu, 2018). Therefore, it was reasonable to use this data to test the new method. In this paper, we only used the vertical derivative of g_{zz} to calculate the depth. The data were provided by Bell Geospace and were gridded in 50-m interval for convenience (Figure 9). The data were processed by bandpass filtering all components between 200 and 5,000 m spatial wavelengths, which aim to remove the regional field from the gradiometer data and to capture the signal associated with the salt body at large, hosting the high-density cap rock. The downward continuation was calculated by using the following parameters: the depth level interval was 20 m, and the maximum depth is set as 600 m. Then we obtained 3D results that were intersected with two cross sections for better visibility. The results are shown in Figure 10. The cross section AA′ is from left to right, and cross section BB′ is from bottom to top. The model tests showed that the new method was able to identify the center depth of the geologic source. Therefore, we can conclude the center depth range of cap rock was 200–400 m. In cross section AA′, the maximum values showed that the center depth ranged from 350 to 200 m. In cross section BB′, the maximum values were located at the depths of 200 and 400 m. This depth ranges corresponded to previous results and drilling information (Salem et al., 2013; Thompson & Eichelberger, 1928). The average depth has been confirmed as 320 m and the depth of cap rock at the southern part is about 200 m and the north to reach 315 m. The results showed that the new method is a useful tool for obtaining depth information and describing the depth ranges of geologic bodies (Geng et al., 2014; Oliveira & Barbosa, 2013; Qin et al., 2019; Salem et al., 2013; Zhou, 2015; Zhou & Liu, 2018).

5. Discussion

The theory section showed that the new method was established using the Taylor series relationship with the continued fraction in space domain. Similar to the downward continuation based on the Taylor series, the continued fraction terms can influence the accuracy of the new method. For the infinite horizontal cylinder model, two terms of continued fraction downward continuation can approach the theoretical formula. For the sphere model, four terms can approach the theoretical formula. When more terms are used, we need use the limiting form to calculate the continued fraction, and the same theoretical formula can be obtained. We cannot use a theoretical formula to denote the complex model or real data. Therefore, we used four terms for calculations in this paper. Based on the tests in the previous sections, we can see that high precision derivatives are important when applying the new method. Some new derivative calculation methods have been proposed to improve accuracy (Fedi & Florio, 2002; Pašteka et al., 2010; Zeng et al., 2015). Meanwhile, a median filter was used to process the results and can be used to decrease the random noise, which is produced by zero or a very small numbers denominator contained in Equation 10. However, to avoid impacts on depth, we only use a 3 × 3 window. In addition, similar to the NTG method, the new method was established based on downward continuation. The depth information can be obtained using the singular (quasi-singular) point directly. Synthetic data with noise showed that the depth estimates could be affected by noise contained in the original data, which therefore needs to be filtered carefully. In comparison with NTG method, therefore, the new method using prisms and sphere models resulted in accurate depth information. This showed that we only need to calculate the downward continuation without calculating the structural index, which also has been proved using the model theory.

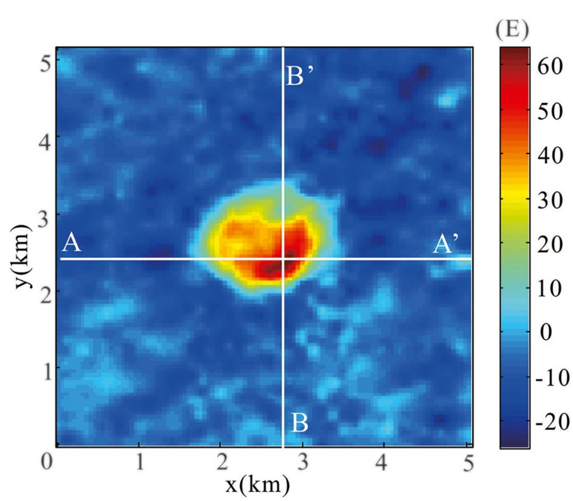

Figure 9. The vertical derivative data from the Vinton Salt Dome, Louisiana, USA.

10.1029/2021EA001789

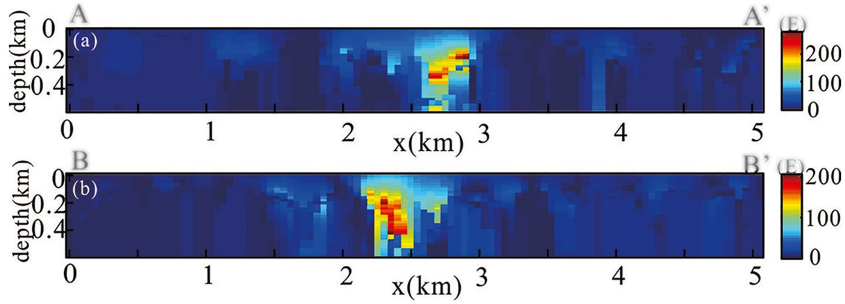

Figure 10. The cross section results of different profiles. (a) Results of AA′ and (b) results of BB′.

6. Conclusions

In this paper, a new downward continuation method was proposed to directly obtain geologic source depth information. The remarkable feature of this method is that it can be utilized to directly estimate the depth based on the downward continuation. We compared the new method with other classical downward continuation methods (such as DCISVD and IDCFFT) and found that similar information could be obtained above the level of the source. At levels below the source, the downward continued data based on the classical method increasing gradually increased with depth. The new method did not display this trend, but rather the position of the singularities can be identified by the maxima near the central position. Therefore, we can use this method to estimate source depth. Theoretically, the singular (quasi-singular) point can be obtained at the source depth using the new method. In practical applications, we only need to calculate downward continuation data from the original level to a maximum depth level and the maximum value can directly be used to indicate the depth information. We used different synthetic models with and without noise to test the new method and compared the results with those based on a normalized total gradient method. For the simple model, both methods obtained satisfactory results. For the complex model, the influence of different sources of error caused inaccurate results. However, the new method had the advantages of higher accuracy and simple calculation procedure. Finally, we used real gravity data to test the new method and results corresponded with the previous results. This illustrated that the new method can be used to calculate the downward continued value above the source. More importantly, it can be used as a new depth estimation method.

Data Availability Statement

Data for this research are not publicly available due to a "Data Licensing Agreement for Non-Commercial Use" of Bell Geospace Inc. need to be signed. But researchers can obtain the data from Bell Geospace Inc. after sign a "Data Licensing Agreement for Non-Commercial Use."

Acknowledgments
We would like to thank Bell Geospace Inc. for the permission to use the real FTG data from the Vinton salt dome. This research was partly supported by the National Natural Science Foundation (42004068, 41904122), China Geological Survey's project (DD20189642, DD20190012, and DD 20190129), the Science and Technology Plan of Gansu Province (20JR5RA251), and the Special Project for Basic Scientific Research Service (JYYWF20180101 and JKY202007).

References

Abbas, M. A., & Fedi, M. (2014). Automatic DEXP imaging of potential fields independent of the structural index. *Geophysical Journal International*, *199*(3), 1625–1632. https://doi.org/10.1093/gji/ggu354

Bastani, M., & Pedersen, L. B. (2001). Automatic interpretation of magnetic dike parameters using the analytical signal technique. *Geophysics*, *66*, 551–561. https://doi.org/10.1190/1.1444946

Cella, F., Fedi, M., & Florio, G. (2009). Toward a full multiscale approach to interpret potential fields. *Geophysical Prospecting*, *57*, 543–557. https://doi.org/10.1111/j.1365-2478.2009.00808.x

Coker, M. O., Bhattacharya, J. P., & Marfurt, K. J. (2007). Fracture patterns within mudstones on the flanks of a salt dome: Syneresis or slumping? *Gulf Coast Association of Geological Societies*, *57*, 125–137.

Cooper, G. R. J. (2006). Interpreting potential field data using continuous wavelet transforms of their horizontal derivatives. *Computers and Geosciences*, *32*, 984–992. https://doi.org/10.1016/j.cageo.2005.10.012

Cuyt, A., & Verdonk, B. (1988). Multivariate reciprocal differences for branched Thiele continued fraction expansions. *Journal of Computational and Applied Mathematics*, *21*, 145–160. https://doi.org/10.1016/0377-0427(88)90264-6

Elysseieva, I. S., & Pašteka, R. (2009). Direct interpretation of 2D potential fields for deep structures by means of the quasi-singular points method. *Geophysical Prospecting*, *57*, 683–705. https://doi.org/10.1111/j.1365-2478.2009.00806.x

Elysseieva, I. S., & Pašteka, R. (2019). Historical development of the total normalized gradient method in profile gravity field interpretation. *Geophysical Prospecting*, *67*, 188–209. https://doi.org/10.1111/1365-2478.12704

Ermokhine, K. M., & Efimova, N. (2006). Analytical continuation of geophysical fields into the area of anomaly sources by the Continued fraction method (CFCM). *In 68th EAGE Conference and Exhibition Incorporating SPE EUROPEC* (p. 324).

Evjen, H. M. (1936). The place of the vertical gradient in gravitational interpretation. *Geophysics*, *1*, 127–136. https://doi.org/10.1190/1.1437067

Fedi, M., & Florio, G. (2002). A stable downward continuation by using ISVD method. *Geophysical Journal International*, *151*, 146–156. https://doi.org/10.1046/j.1365-246x.2002.01767.x

Fedi, M., & Florio, G. (2011). Normalized downward continuation of potential fields within the quasi-harmonic region. *Geophysical Prospecting*, *59*, 1087–1100. https://doi.org/10.1111/j.1365-2478.2011.01002.x

Fedi, M., Florio, G., & Cascone, L. (2012). Multiscale analysis of potential fields by a ridge consistency criterion: The reconstruction of the Bishop basement. *Geophysical Journal International*, *188*, 103–114. https://doi.org/10.1111/j.1365-246x.2011.05259.x

Fedi, M., Florio, G., & Paoletti, V. (2015). MHODE: A local homogeneity theory for improved source-parameter estimation of potential fields. *Geophysical Journal International*, *202*, 887–900. https://doi.org/10.1093/gji/ggv185

Fedi, M., Florio, G., & Quarta, T. (2009). Multiridge analysis of potential fields: Geometrical method and reduced Euler deconvolution. *Geophysics*, *74*, L53–L65. https://doi.org/10.1190/1.3142722

Florio, G., & Fedi, M. (2014). Multiridge Euler deconvolution. *Geophysical Prospecting*, *62*, 333–351. https://doi.org/10.1111/1365-2478.12078

Florio, G., & Fedi, M. (2018). Depth estimation from downward continuation: An entropy based approach to normalized full gradient. *Geophysics*, *83*, J33–J42. https://doi.org/10.1190/geo2016-0681.1

Geng, M. X., Huang, D. N., Yang, Q. J., & Liu, Y. P. (2014). 3D inversion of airborne gravity-gradiometry data using cokriging. *Geophysics*, *79*, G37–G47. https://doi.org/10.1190/geo2013-0393.1

Gupta, O. P. (1983). A least-squares approach to depth determination from gravity data. *Geophysics*, *48*, 357–360.

Hansen, R. O. (2005). 3D multiple-source Werner deconvolution for magnetic data. *Geophysics*, *70*, L45–L51. https://doi.org/10.1190/1.2073883

Hartman, R. R., Teskey, D. J., & Friedherg, J. L. (1971). A system for rapid digital aeromagnetic interpretation. *Geophysics*, *36*, 891–918. https://doi.org/10.1190/1.1440223

Jackson, M. P. A., Roberts, D. G., & Snelson, S. (1995). *Salt tectonics: A global perspective* (Vol. 65). AAPG, Memoir 65. https://doi.org/10.1306/M65604

Keating, P. (2009). Improved use of local wavenumber in potential filed interpretation. *Geophysics*, *74*, 75–85. https://doi.org/10.1190/1.3242270

Lee, J., & Kim, D. H. (2011). Simple high-order approximations for unsteady-state diffusion, adsorption and reaction in a catalyst: A unified method by a continued fraction for slab, cylinder and sphere geometries. *Chemical Engineering Journal*, *173*, 644–650. https://doi.org/10.1016/j.cej.2011.08.029

Li, S. F., & Chen, D. D. (2015). Comparative study on computing effect of continued fraction approximation and polynomial approximation. *Journal of Bengbu University*, *4*, 29–31 (in Chinese with English abstract).

Li, S. F., Tan, J. Q., Xie, C. J., & Li, L. (2008). An iterative formula with four order convergence for solving equations based on Thile's continued fraction. *Journal of University of Science and Technology of China*, *38*, 138–140 (in Chinese with English abstract).

Li, X. (2003). On the use of different methods for estimating magnetic depth. *The Leading Edge*, *22*(11), 1090–1099. https://doi.org/10.1190/1.1634912

Lim, J. S. (1990). *Two-dimensional signal and image processing* (pp. 469–476). Englewood Cliffs, NJ: Prentice Hall.

Ma, G. Q., Liu, C., Huang, D. N., & Li, L. L. (2013). A stable iterative downward continuation of potential field data. *Journal of Applied Geophysics*, *98*, 205–211. https://doi.org/10.1016/j.jappgeo.2013.08.018

Nabighian, M. N. (1972). The analytic signal of two dimensional magnetic bodies with polygonal cross-section—Its properties and use of automated anomaly interpretation. *Geophysics*, *37*, 507–517. https://doi.org/10.1190/1.1440276

Naudy, H. (1971). Automatic determination of depth on aeromagnetic profiles. *Geophysics*, *36*, 717–722. https://doi.org/10.1190/1.1440207

Oliveira, V. C., & Barbosa, V. C. F. (2013). 3-D radial gravity gradient inversion. *Geophysical Journal International*, *195*, 883–902. https://doi.org/10.1093/gji/ggt307

Pašteka, R., Karcol, R., Kušnirák, D., & Mojzeš, A. (2012). REGCONT: A MATLAB based program for stable downward continuation of geophysical potential fields using Tikhonov regularization. *Computers and Geosciences*, *49*, 278–289.

Pašteka, R., Richter, F. P., Karcol, R., Brazda, K., & Hajach, M. (2010). Regularized derivatives of potential fields and their role in semi-automated interpretation methods. *Geophysical Prospecting*, *57*, 507–516.

Pilkington, M., & Boulanger, O. (2017). Potential field continuation between arbitrary surfaces—Comparing methods. *Geophysics*, *82*, J9–J25. https://doi.org/10.1190/geo2016-0210.1

Qin, P. B., Xiang, M., Liang, X., & Hou, Z. L. (2019). A new method to integrate different gravity gradient components in reweighted regularized inversion with a minimum support constraint. *Geophysical Journal International*, *217*, 1387–1412.

Roest, W. R., Verhoef, J., & Pikington, M. (1992). Magnetic interpretation using the 3-D analytic signal. *Geophysics*, *57*(1), 9–210. https://doi.org/10.1190/1.1443174

Salem, A., Masterton, S., Campbell, S., Fairhead, J. D., Dickinson, J., & Murphy, C. (2013). Interpretation of tensor gravity data using an adaptive tilt angle method. *Geophysical Prospecting*, *61*, 1065–1076. https://doi.org/10.1111/1365-2478.12039

Stavrev, P., & Reid, A. (2007). Degrees of homogeneity of potential fields and structural indices of Euler deconvolution. *Geophysics*, *72*, L1–L12. https://doi.org/10.1190/1.2400010

Stavrev, P., & Reid, A. (2010). Euler deconvolution of gravity anomalies from thick contact/fault structures with extended negative structural index. *Geophysics*, *75*, I51–I58. https://doi.org/10.1190/1.3506559

Thompson, D. T. (1982). EULDPH: A new technique for making computer assisted depth estimates from magnetic data. *Geophysics*, *47*, 31–37. https://doi.org/10.1190/1.1441278

Thompson, S. A., & Eichelberger, O. H. (1928). Vinton salt dome, Calcasieu Parish, Louisiana. *AAPG Bulletin*, *12*, 385–394. https://doi.org/10.1306/3d9327ec-16b1-11d7-8645000102c1865d

Thurston, J. B., & Smith, R. S. (1997). Automatic conversion of magnetic data to depth, dip, and susceptibility contrast using the SPI (TM) method. *Geophysics*, *62*, 807–813. https://doi.org/10.1190/1.1444190

Wang, Y. G., Zhang, F. X., Wang, Z. W., Meng, L. S., & Zhang, J. (2011). Taylor series iteration for downward continuation of potential fields. *Oil Geophysical Prospecting*, *46*(4), 657–662 (in Chinese with English abstract).

Xu, S. Z., Yang, J. Y., Yang, C. F., Xiao, P. F., Chen, S. C., & Guo, Z. H. (2007). The iteration method for downward continuation of a potential field from a horizontal plane. *Geophysical Prospecting*, *55*, 883–889. https://doi.org/10.1111/j.1365-2478.2007.00634.x

Zeng, H. L., Meng, X. H., Yao, C. L., Li, X. M., Lou, H., Guan, Z. N., & Li, Z. P. (2002). Detection of reservoirs from normalized full gradient of gravity anomalies and its application to Shengli oil field, east China. *Geophysics*, *67*, 1138–1147. https://doi.org/10.1190/1.1500375
Zeng, X. N., Li, X. H., Jia, W. M., & Liu, D. Z. (2015). A new regularization method for calculating the vertical derivatives of the potential field. *Chinese Journal of Geophysics*, *58*, 1400–1410.
Zeng, X. N., Li, X. H., Su, J., Liu, D. Z., & Zou, H. X. (2013). An adaptive iterative method for downward continuation of potential-field data from a horizontal plane. *Geophysics*, *78*, J43–J52. https://doi.org/10.1190/geo2012-0404.1
Zhang, C., Lü, Q., Yan, J. Y., & Qi, G. (2018). Numerical solutions of the mean-value theorem: New methods for downward continuation of potential fields. *Geophysical Research Letters*, *45*, 3461–3470. https://doi.org/10.1002/2018GL076995
Zhang, H. L., Ravat, D., & Hu, X. Y. (2013). An improved and stable downward continuation of potential field data: The truncated Taylor series iterative downward continuation method. *Geophysics*, *78*, J75–J86. https://doi.org/10.1190/geo2012-0463.1
Zhou, W. N. (2015). Normalized full gradient of full tensor gravity gradient based on adaptive iterative Tikhonov regularization downward continuation. *Journal of Applied Geophysics*, *118*, 75–83. https://doi.org/10.1016/j.jappgeo.2015.04.012
Zhou, W. N. (2016). Depth estimation method based on the ratio of gravity and full tensor gradient invariant. *Pure and Applied Geophysics*, *173*, 499–508. https://doi.org/10.1007/s00024-015-1117-7
Zhou, W. N., Li, J. Y., & Yuan, Y. (2018). Downward continuation of potential field data based on Chebyshev–Padé approximation function. *Pure and Applied Geophysics*, *175*, 275–286. https://doi.org/10.1007/s00024-017-1680-1
Zhou, W. N., & Liu, C. Y. (2018). Depth from extreme points method for gravity gradient tensor data. *Geophysical Prospecting*, *66*, 432–443. https://doi.org/10.1111/1365-2478.12512
Zhou, W. N., Nan, Z. Y., & Li, J. Y. (2016). Self-constrained Euler deconvolution using potential field data of different altitudes. *Pure and Applied Geophysics*, *173*, 2073–2085. https://doi.org/10.1007/s00024-016-1254-7